Yu et al, Fig. S1

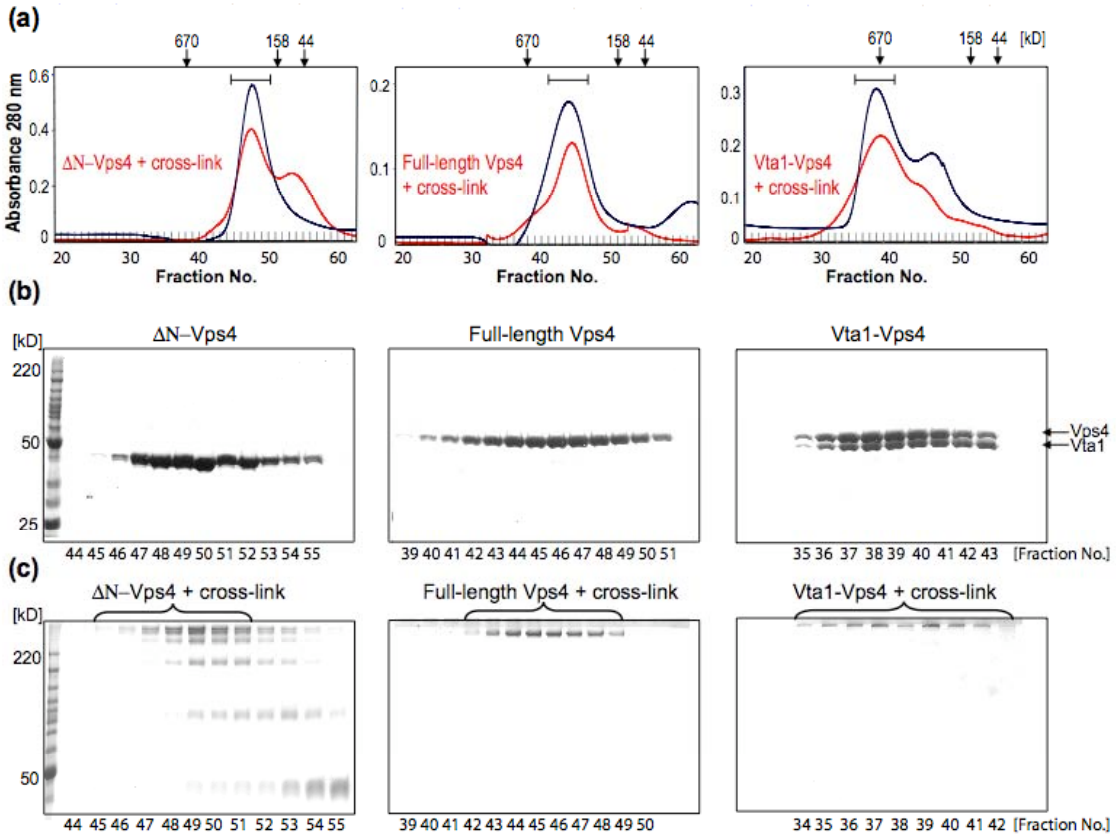

Fig. S1. Analyses of glutaraldehyde-crosslinked Vps4p complexes. SDS-PAGE analyses of assembled ΔN-Vps4p (left panels), full length Vps4p (middle panels), and Vta1-Vps4p (right panels) complexes before and after cross-linking with glutaraldehyde. **A)** Assembled complexes were analyzed by Superose 6 size–exclusion chromatography in 1 mM ATP (black traces). Peak fractions (square brackets) were glutaraldehyde crosslinked, concentrated and rechromatographed without ATP (red traces). **B and C**) Peak fractions from assembled (**B**) or crosslinked (**C**) samples were analyzed by SDS-PAGE, with Coomassie blue staining. Bracketed fractions in (**C**) were pooled and imaged by cryoEM.

Yu et al, Fig. S2

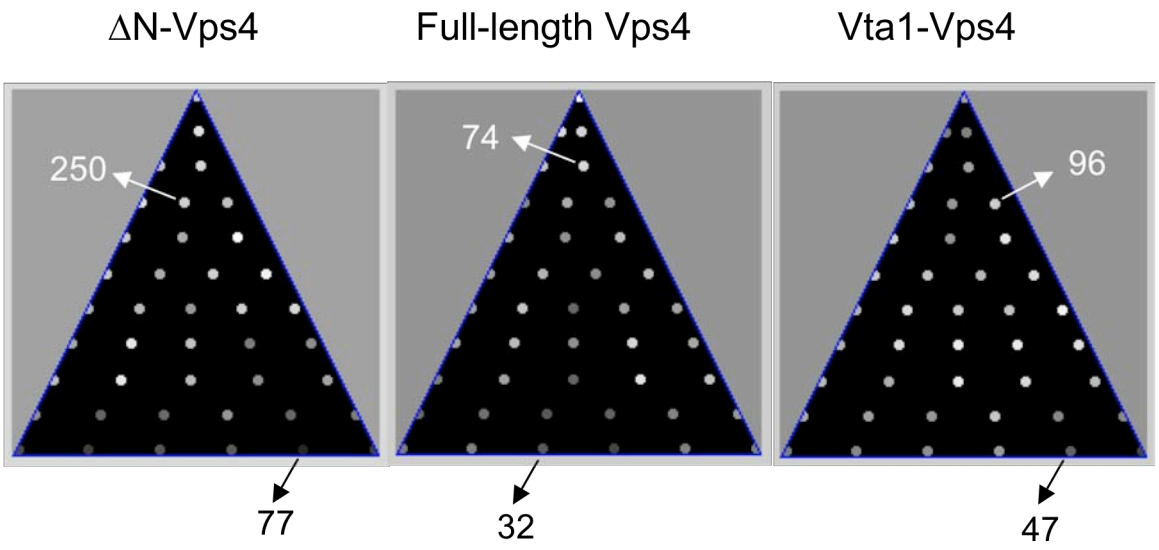

Fig. S2. Euler angle distributions for the three reconstructions. The relative intensity of each dot indicates the number of particles in that orientation (class). The highest and lowest numbers of particles represented are shown. This figure was generated by the *eman* program in the EMAN software package.

Yu et al, Fig. S3

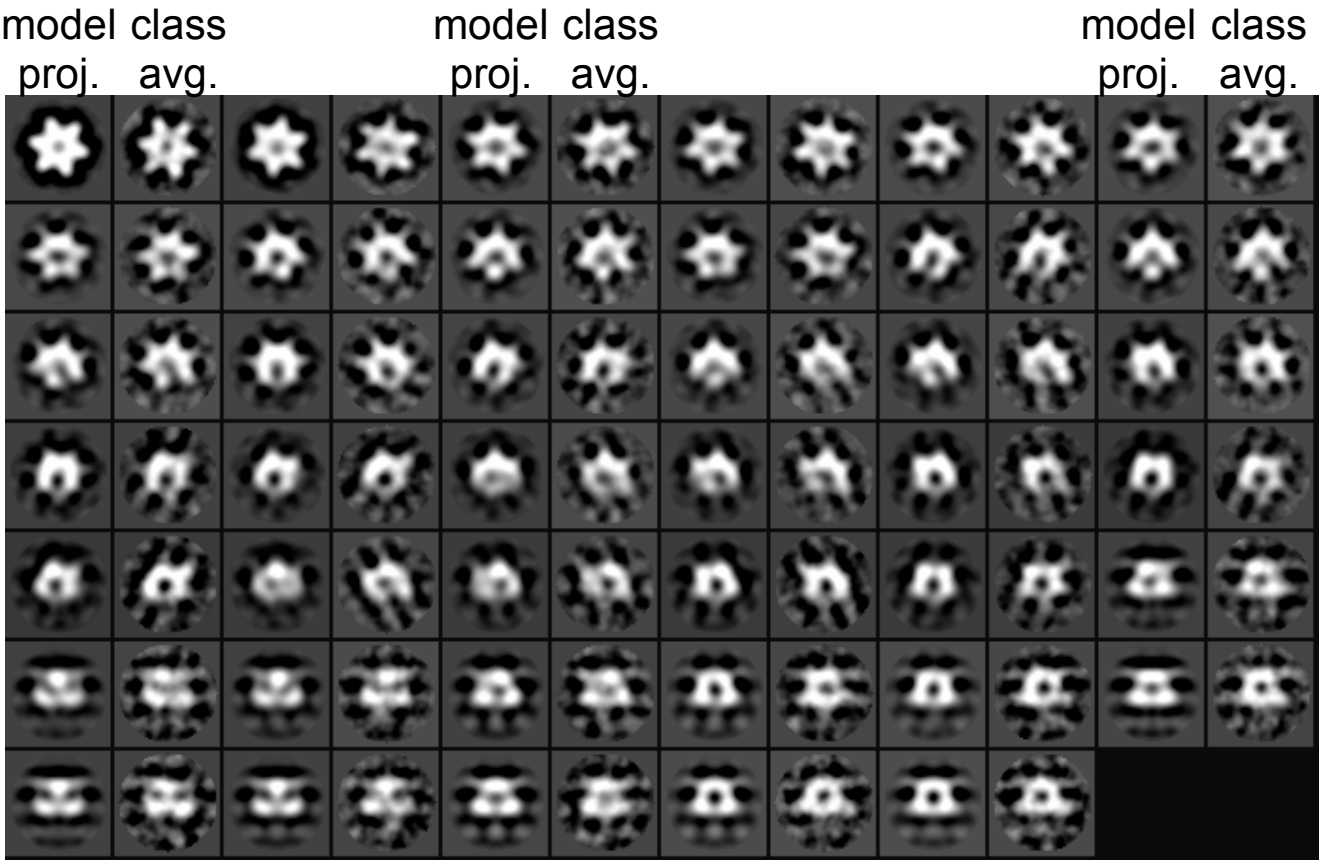

Fig. S3. Model projections and class averages (in alternating columns) for the final reconstruction of ΔN-Vps4p.

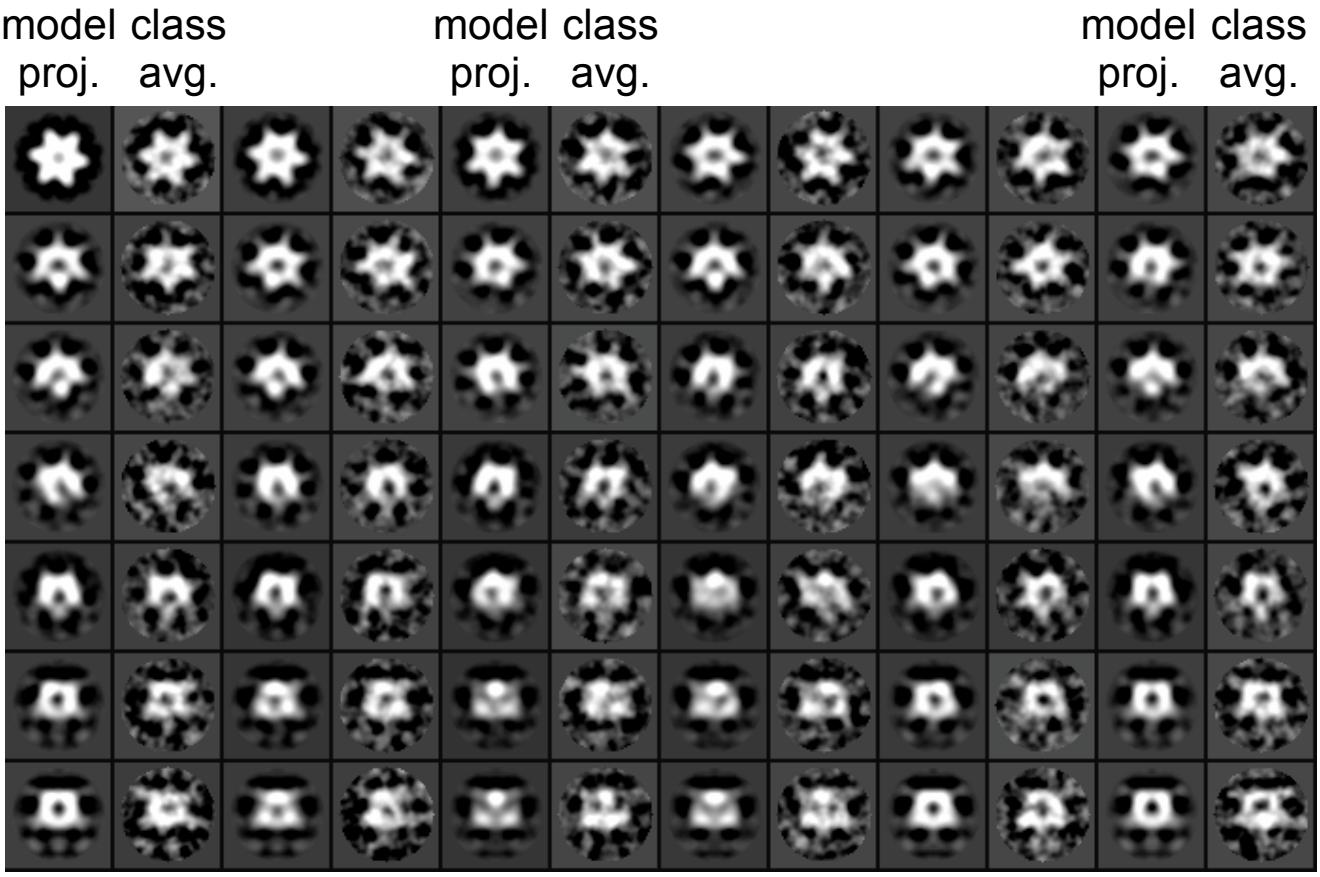

Fig. S4. Model projections and class averages (in alternating columns) for the final reconstruction of full-length Vps4p.

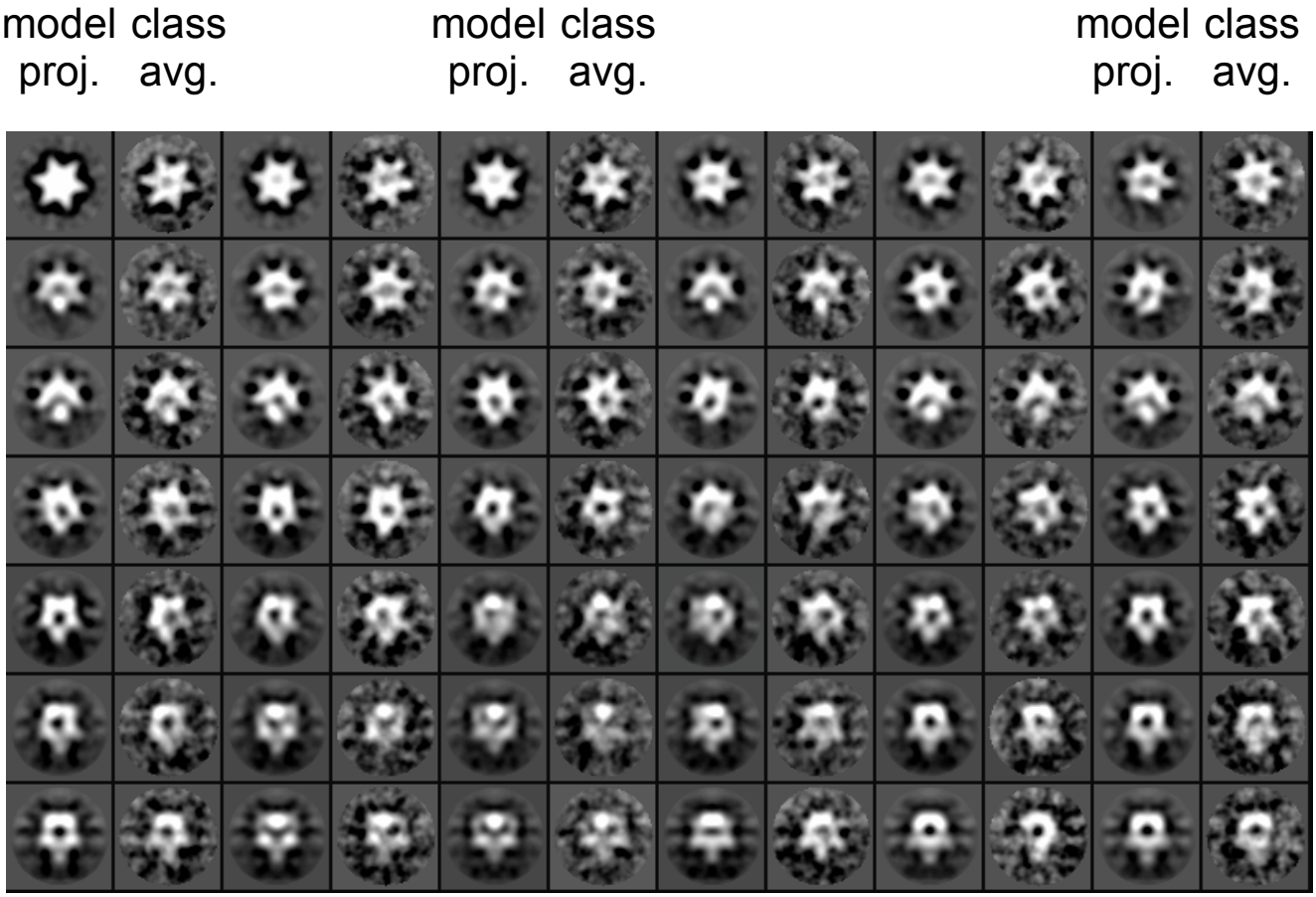

Fig. S5. Model projections and class averages (in alternating columns) for the final reconstruction of Vta1p-Vps4p.

Yu et al, Fig. S6

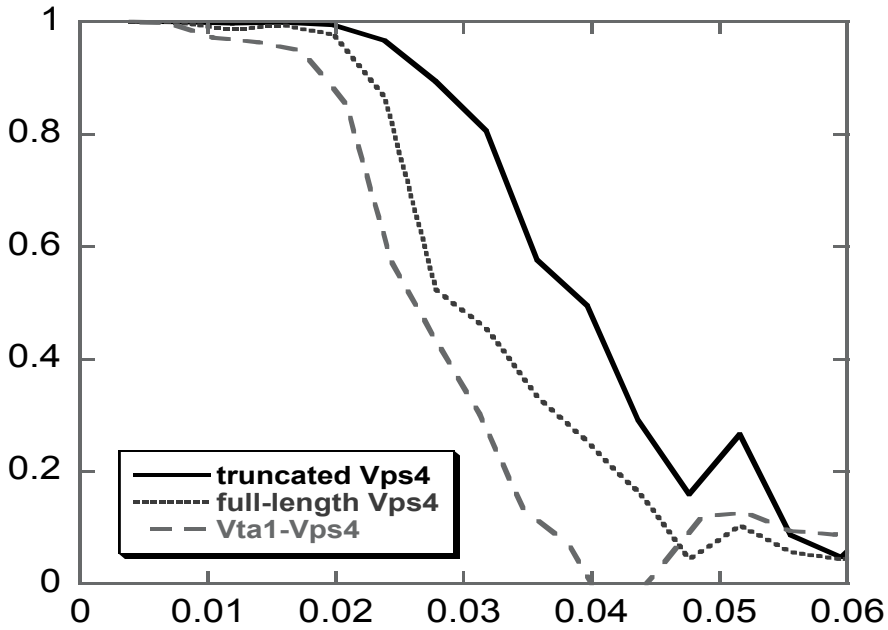

Fig. S6. Fourier shell correlation (FSC) curves. The estimated resolutions (FSC = 0.5) are 25 Å, 34 Å and 38 Å for the ΔN-VPS4p, full-length Vps4p and Vta1p-Vps4p complexes, respectively. The N-terminal domain of Vps4p is responsible for recruiting substrates and contains an MIT domain and a long linker. It is therefore likely to be at least partially disordered. The adaptor protein Vta1p also participates in substrate binding and appears to be mostly disordered in solution (Wes Sundquist, unpublished). Thus the resolutions obtained correlate with the expected degree of disorder.

Yu et al, Fig. S7

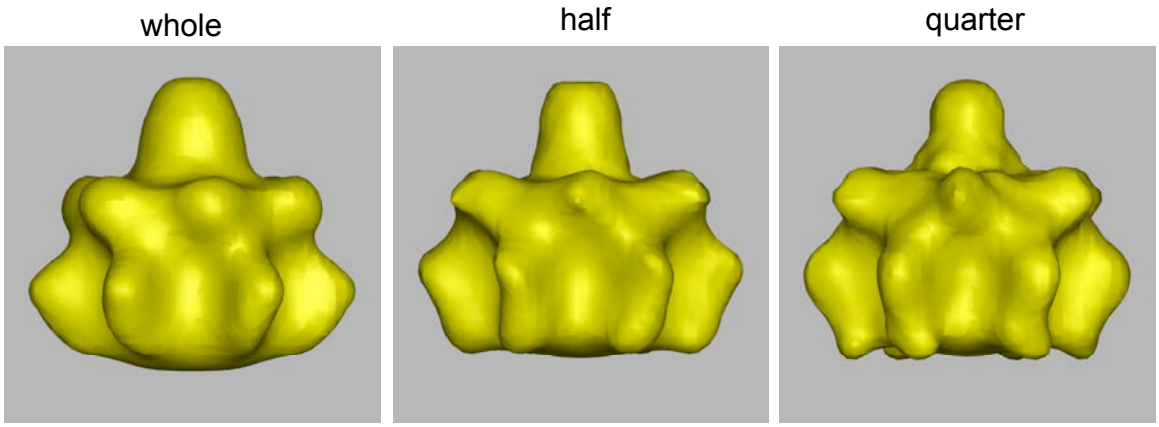

Fig. S7. Resolution is limited by particle heterogeneity, not the number of images included. Vta1-Vps4 reconstructions using all, half, and a quarter of the images are shown, all contoured at 824 kDa. Even the quarter-data-set reconstructions converged, as indicated by the clear similarity of model projections and final class averages. The resolution, as assessed by comparing the two half-data sets was 38 Å (one data point), while the six independent comparisons of quarter-data sets yielded resolutions just slightly worse, between 39-41 Å. Thus the heterogeneity of the particles, rather than the total number of images included, is the principle resolution limitation.

Yu et al, Fig. S8

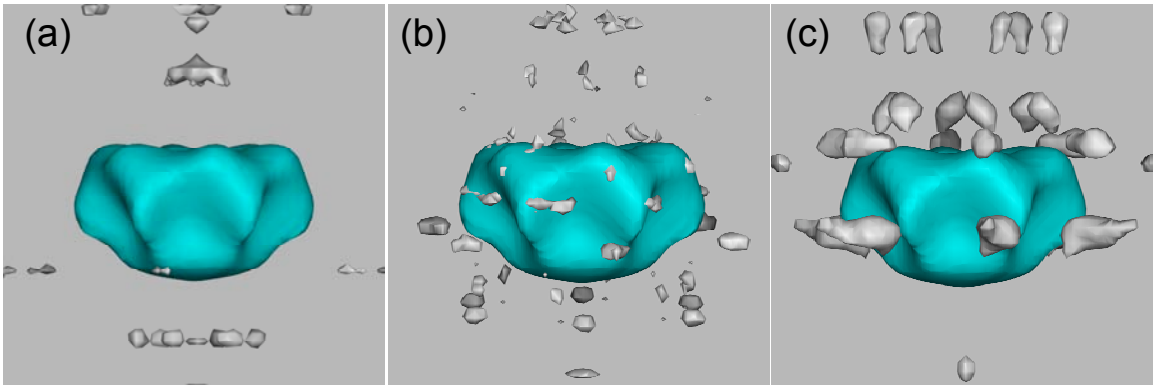

Fig. S8. "Control" difference maps between half-data-set reconstructions of (a) ΔN-Vps4p, (b) full-length Vps4p and (c) Vta1p-Vps4p complexes, respectively, contoured at 3.5 σ, consistent with Fig. 7 of the main text.

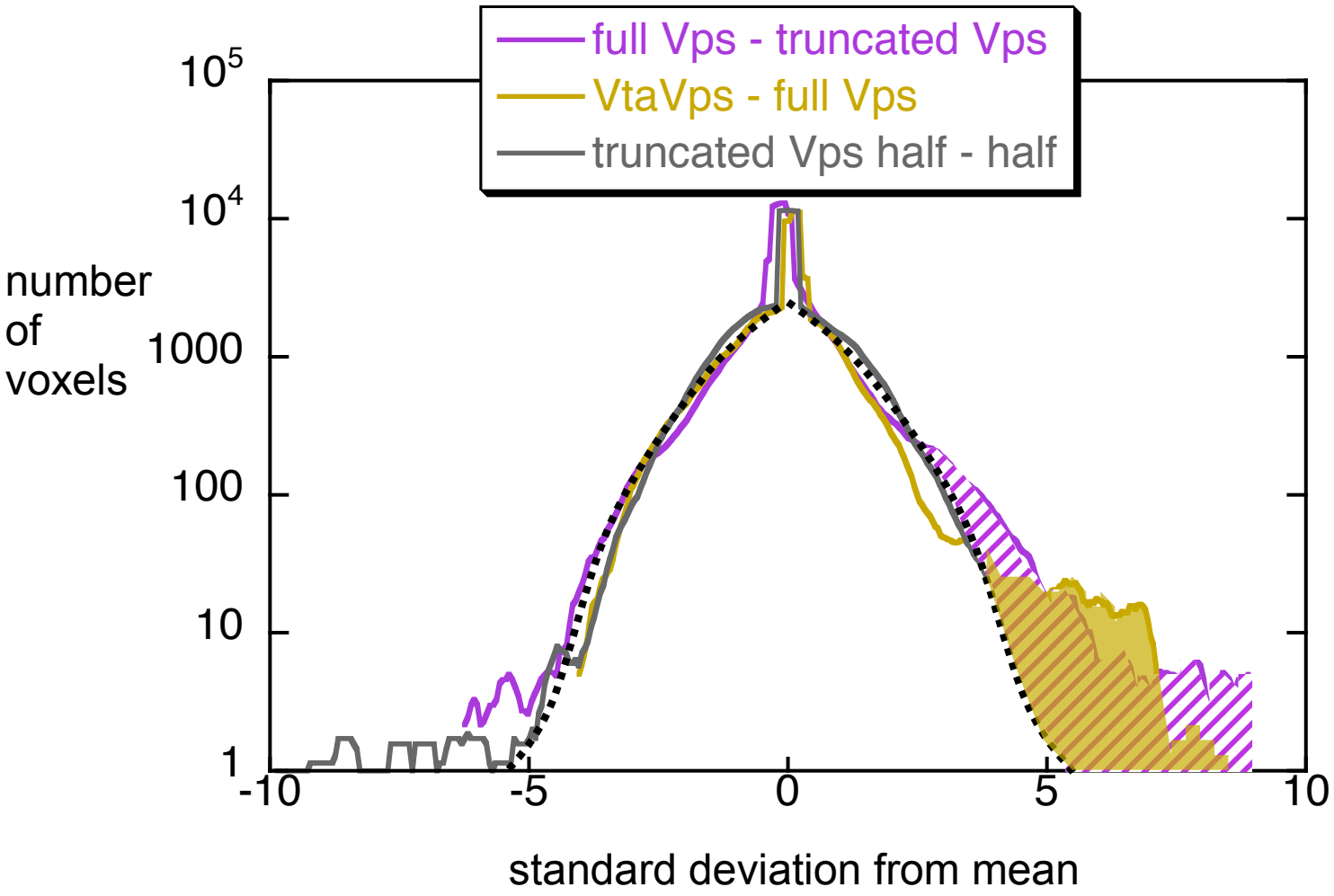

Fig. S9. Difference map histograms. Differences arise from the presence of additional protein mass, conformational changes, or noise. Unlike positive differences due to new protein, positive differences due to conformational changes and noise should be accompanied by corresponding negative differences. Thus the histogram for the "control" difference map between the two ΔN-VPS4p half-data-set reconstructions exhibited a monotonic symmetric peak around zero extending to approximately ±5σ. In sharp contrast, the other two difference maps (full-length Vps4p minus ΔN-VPS4p and Vta1p-Vps4p minus full-length Vps4p) had large shoulders of positive differences beyond +3.5σ which are not matched by corresponding negative differences and which reflect the presence of authentic additional densities.